Microwave and HF Multi-Frequency Radars
For Dual-Use Coastal Remote Sensing Applications

Dennis B. Trizna, Lillian Xu
Imaging Science Research, Inc.
9310A Old Keene Mill Road
Burke, VA 22015, USA
dennis@isr-sensing.com

INTRODUCTION

By nature of their transmit frequencies and typical available bandwidths, the use of microwave, VHF and HF radars to measure coastal ocean properties offers sensing scale capabilities at 10m, 100 m, and 1 km, respectively. Similarly, spatial coverage for these three groups typically span 2 km, 5-20 km, and 20-200 km, determined by radar echo strengths and propagation loss for each frequency range. Only HF radar signals can propagate reliably beyond the horizon, because the salty ocean water has sufficient conductivity to support the surface wave mode at HF. Ocean wave spectra are typically homogeneous over all of these scales (except, perhaps, at the longest coverage afforded by HF band) so that maps of ocean wave spectra are typically not practical. At the smallest scales and nearest the coast, rips currents and coastal shear waves have structure at the 10-m scale and extend to a few hundred meters off shore, and are thus amenable to coherent microwave sensing. River outflow plumes and eddies have scales and ranges appropriate to VHF radars, while large eddies and tidal flows typically are mapped by HF radars. More importantly, HF radars covering the entire 3-30 MHz band simultaneously can measure current shear between 0.40 and 4.0-m depth, not practical by any other means at 1-km scales. We discuss a new capability to achieve sensing at all of these scales, making use of digital transceiver / receiver technology that is applied over these three radar frequency bands.

DIGITAL TRANSCEIVER TECHNOLOGY

ISR has developed a family of digital transceivers and receivers, based on PC PCI board technology, that support the multiple radar requirements discussed above. This family is based upon a transceiver with 100 MHz bandwidth, fully programmable pulse forming that includes pulse shaping, phase coding, and frequency modulation, that can be applied directly at VHF and HF, and that can be mixed with a coherent microwave source for use as a coherent microwave imaging radar. This transceiver (the *Octopus*) is designed with an on-board programmable exciter, capable of simple pulse, FMCW, phase coding, variable pulse length and pulse-repetition-frequency; eight receive channels, with the ability to sum up to 256 consecutive waveforms on the board to achieve up to 16-bit samples; an on-board GPS receiver supporting bistatic operation for precise timing. The *Octopus* is used in our HF radar line as the basis of 4 to16-element array radar.

Other members of this family based on the same board design include an 8-channel receive-only card, for use in 16 and 32 element arrays *(OctRec)*; an exciter card for bistatic transmission, where the receive channels have been eleiminated (*Exciter*); a 4-channel receiver card (*QuadRec*) for marine radar applications; and the *Quadrapus*, a 4-channel transceiver, for our coherent microwave radar in development.

MICROWAVE RADAR SENSING

Use of a non-coherent marine radar for ocean wave spectra measurement is feasible by making use of multiple-rotation images, and 3-D FFT image processing to derive Ω–K ocean wave spectra [1, 2]. We have developed such a capability, based on the Sitex family of marine radars. Figs. 1a and 1b show wave images and 2 of 16 derive Ω–K components.

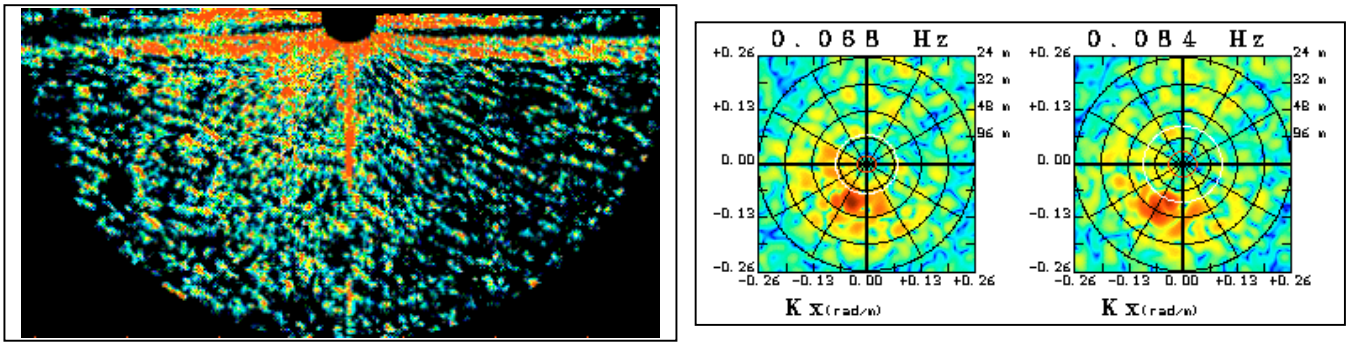

Figure 1a, b. Radar images of ocean waves at the FRF pier, Duck, N.C. ; two K-spectra for frequencies 0.68 and 0.84 Hz derived from such a radar image using 3D-FFT processing of 32 consecutive radar images.

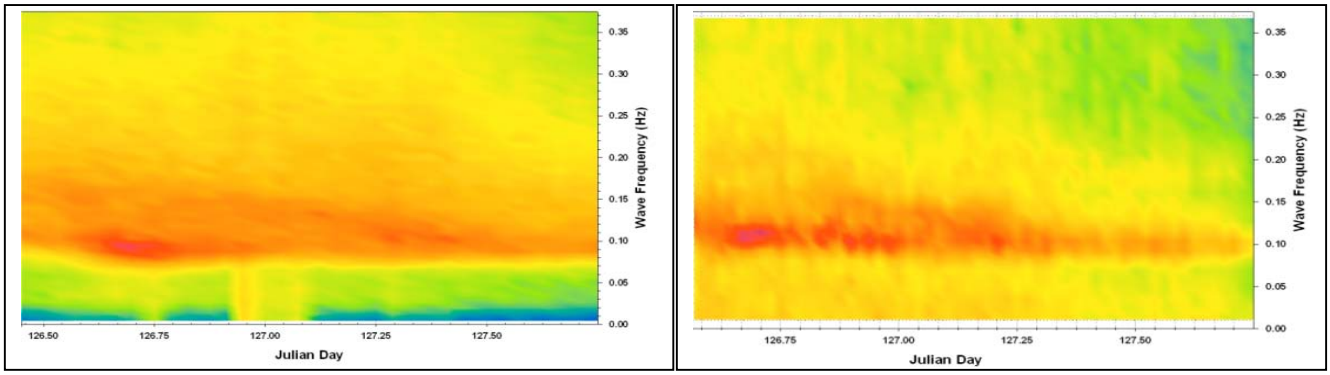

Figure 2. Buoy frequency time series (left) from 3 miles offshore and radar-derived wave spectral time series from ~500 m offshore both capture the same spectral characteristics of a high wave event ocurring during May 2005.

The radar used for the analysis is the ISR Digital Imaging Radar Model 25.9, based on a modified SiTex 25-kWatt 9' antenna system, with our digital acquisition system and signal processing systems, RIPS and RADDS. Wave images from this radar are captured each 1.36-s rotation in double speed mode, and square windows are captured for 3D-FFT analysis. A sequence of 32 such images produces 16 positive frequencies, as well as 16 redundant negative frequencies as the input images are real values and not complex. The peaks in such K-spectra in Fig. 1b locate the direction of energy, and are found empirically to be proportional to the wave height spectral component, the ratio being the modulation transfer function (MTF). Results from such an analysis are shown in Fig. 2, comparing a time series of ocean wave frequency spectra from a buoy three miles off shore with radar derived spectra 500 m off shore. Differences are attributed to shoaling effects as the waves move into shallow water, dissipating energy at the longest wavelengths and shortest frequencies.

This radar system is in final stages of testing and calibration of wave height spectra against surface truth is underway. The radar can be mounted in an unattended van with solar powered batteries, radio network for data transfer to a host site. A variety of GUI interface output results are in final design and will be reported upon in the near future. A coherent version of this radar is in development. From orbital wave images and Ω-K spectra, we will obtain directional wave spectra directly, without an MTF. Of equal importance, we will be able to map surface current vectors with a pair of such systems spaced roughly one km apart, providing maps of rip currents and channel currents for shipping.

HF MULTI-FREQUENCY RADAR

Broad Band Log-Periodic Transmit and Receive Arrays

A new radar antenna was designed for broad band operation over the entire 3-30 MHz band, a modified Log-Periodic Array (LPA) antenna, shown in Fig. 3 deployed at the USACE FRF field test site. However, more compact designs are feasible for operation at pre-specified selected frequencies of four or eight in number, say for operational current shear maps. Th LPA provides full tunability to any frequency in the HF band, and is suggested for target classification applications, or current shear experiments.

The receive antenna array is based on a loop design, three of which are shown in Fig. 3. ISR internal broad preamplifiers provide impedance matching to the loop over the 3-30 MHz filtered output. These elements can be arranged for Direction-of-Arrival (DOA) processing. A small 4-element loop array requires less space than long linear arrays, and is useful for current mapping and ship classification, but cound not be used for measurement of directional wave spectra. For this latter application, long arrays of between 8 and 32 elements, in groups of 8, can be built using an Octopus transceiver, supported by up to three OctRec cards, all of which are time-locked to the master clock on the Octopus card.

Figure 3. HF transmit LPA antenna and 4-element loop receive array for 3-30 MHz operation.

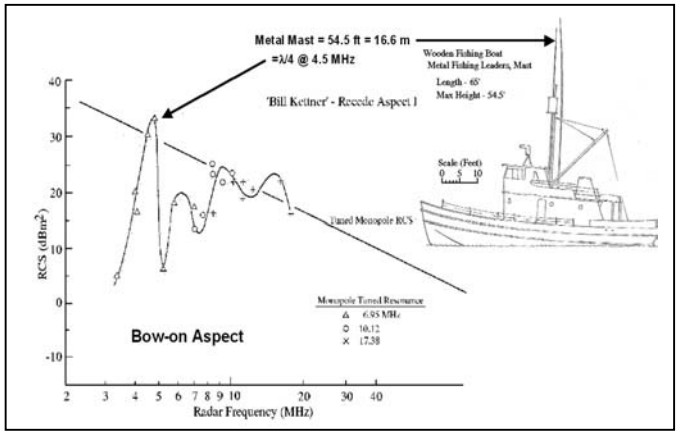

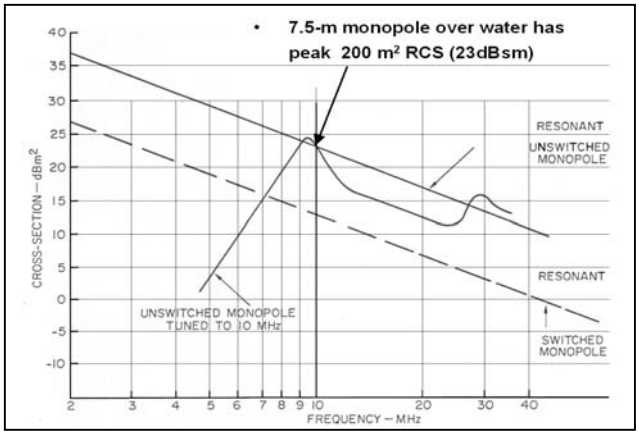

Figure 4a & b. Radar cross section vs. HF frequency shows a maximum correcsponding to resonant monopole contribution from metal ship mast. Calibrated monopole RCS for resonant 7.5-m high monopole over a ground screen.

SHIP TARGET CLASSIFICATION USING MULTIPLE-FREQUENCY HF RADAR

Multi-frequency RCS Ship Measurements

Experiments conducted in the 1970's by an NRL team that included the author demonstrated that ship and small boat targets have a RCS 'spectroscopic fingerprint' across the 3-30 MHz HF band. Fig 4a shows an example of data from that report [3] using a commercial fishing boat target over 3-20 MHz. These data were collected using a tuned resonant monopole as an RCS reference, so that the RCS was determined relative to that calibration. This approach was repeated, retuning the monopole to a different height each time, and is more reliable than trying to solve the radar equation.

In addition to the bulkhead, the other metal structures, such as the mast and fishing leader lines hanging vertically from the stowed fishing gear, could act as vertical monopole scattering elements, contributing to higher frequency peaks. The mast was the tallest element at 16.6 m high, corresponding to a quarter wavelength monopole resonant radar frequency, F_R, equal to 4.5 MHz, in good agreement with the measurements. The RCS for a 7.5-m monopole is shown in Fig. 3b.

Muliple Monopole Ship RCS Model

Figure 5a shows the geometry for a bistatic scattering condition for two monopoles spaced by a distance, L, seen in plan view. Each has a respective scattering cross section σ_1 and σ_2, and each is a function of radar frequency. The illuminator generates a surface mode plane wave along a propagation direction separated from the scattered direction to the receive array by bistatic angle, Φ_B. The aspect of the target's course heading relative to the receive array is Φ_A. Since the monopole RCS is omni-directional, the scattered fields will add with a phase difference that is only function of the difference in phase path.

A simple two-mast model based on monopoles resonant at 8 and 12 MHz and spaced 7.5 m apart was used to generate the bistatic received power as a function of bistatic angle. The curve of Figure 4b was taken and scaled to arbitrary resonant frequency, producing appropriate frequency dependent RCS for any quarter wavelength selected. The bistatic RCS was calculated for this geometry and is shown in Fig. 5b below.

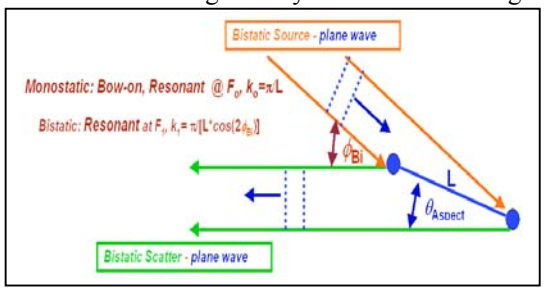

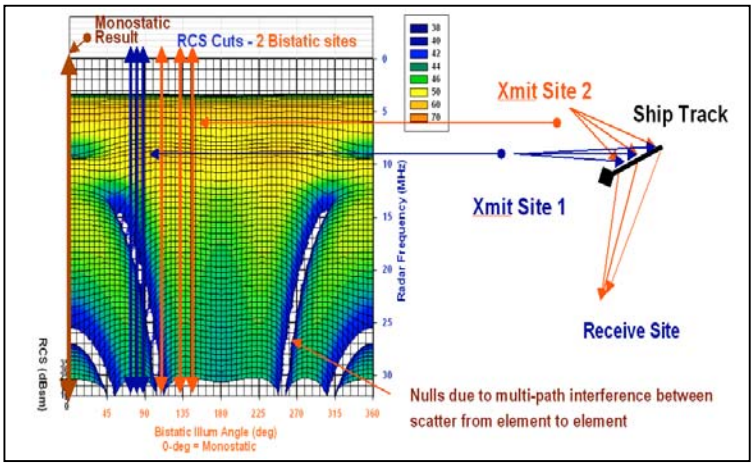

Figure 5a & b. Geometry for scatter from a two-monopole ship model (e.g., double-mast sailing boat) ; bistatic RCS shows peaks and nulls that can be used as classification markers using a multiplicity of angles and frqeuencies.

Ship Classification using Multiple Frequencies

An example of how data for comparison with such a model would be used for classification is shown in Figure 5b for a ship represented by a monopole-pair model. The radar illumination plan-view geometry is shown to the right for two bistatic sources, Site 1 and 2, with the receiver site below. The three sets of blue and red lines over the RCS surface represent scatter paths for three positions of the target moving from right to left, the diamond representing the ship's bow. These three boat locations generate three samples of bistatic RCS vs. frequency for each site, as indicated by the 3 blue and red vertical lines over the RCS plot to the left, as if one had continuous frequency coverage over the HF band. In practice, 30 frequencies are more likely, so that discrete samples would be occur along these lines to generate a matrix of frequency-bistatic-angle samples for target classification. Both the maxima and deep minima would be used as the classifiers, with accuracy of classification increasing with greater number of aspect angle samples, and/or bistatic transmitter sources. The goal is to sample as many locations as possible in the frequency-aspect angle domain. Of course algorithms to classify would require development to achieve a robust classification tool.

MULTIPLE- FREQUENCY CURRENT SHEAR MEASURENTS

Use of multiple frequencies allows one to map currents versus depth, [4, 5, 6]. With HF low radar frequencies and modest wind speed, one can measure currents below the wind driven surface shear layer to identify other ambient currents not driven by the wind. Some results representing such a condition are presented next. We recently conducted a ship RCS experiment using 32 frequencies covering the HF band and a depth range equivalent to 0.4 to 4 meters (~ 8% of Bragg resonant ocean wavelength, or 4% of radar wavelength). Four loop antenna elements identical to those shown in Figure 3 were used in a linear receive array. These data were collected at a U.S. Navy field site off the coast of Pt. Loma, California. The Doppler spectra were extremely broad, indicating a complex current field in the immediate vicinity off shore. We submitted these spectra to our proprietary direction-of-arrival analysis that is used to track targets on course to verify their identification from other ship traffic in the area. The results of the radial Doppler shift that we found are summarized in Fig. 6. Data for the lowest frequencies were somewhat noisy, so we used a depth of three meters as the deep-water cutoff in the display. Doppler shifts are plotted for 12^o interpolated increments covering a total of 60^o of coverage, as the direction-of-arriveal (DOA) method provides discrete angles as solutions with uneven spacing. Negative angle is clockwise relative to 245^o boresight.

The radial velocity profile becomes complicated between about 50 cm and one meter and is quite noisy. This is assumed to be due to the chaotic transition from the surface layer wind driven current to a current field that appears to be due to a local gyre or eddy passing by. The deeper water structure below one meter indicates a consistent clock-wise eddy structure roughly centered in front of the receive antenna boresite (0^o local, 245^o true). At the rightmost bearing, -36^o, the radial current is a maximum over most depths. Below two meters, the relative radial magnitudes change sense, as one might expect if the eddy were tilted, similar to a tornado at lower levels. As one considers bearings running to the left approaching boresight, the radials decrease in magnitude and approach zero between boresight and –12 deg.

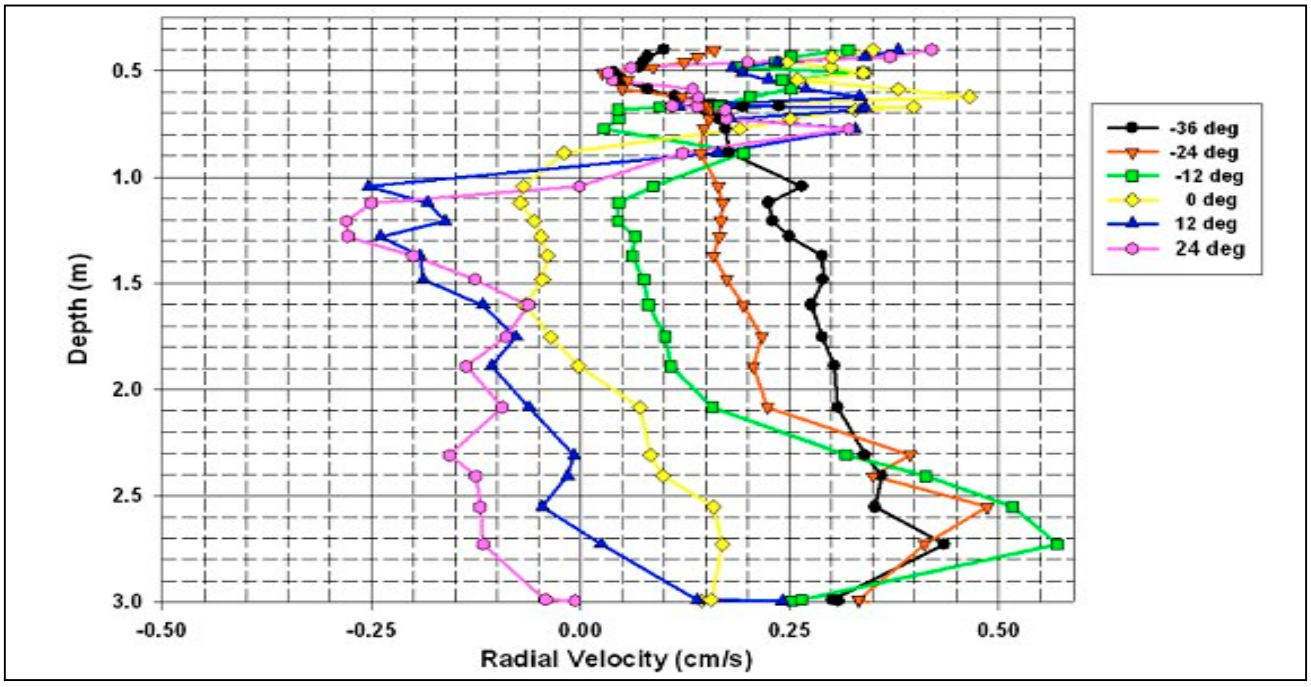

Figure 6. Current shear profiles using 30 frequencies show difference in surface and deep water currents.

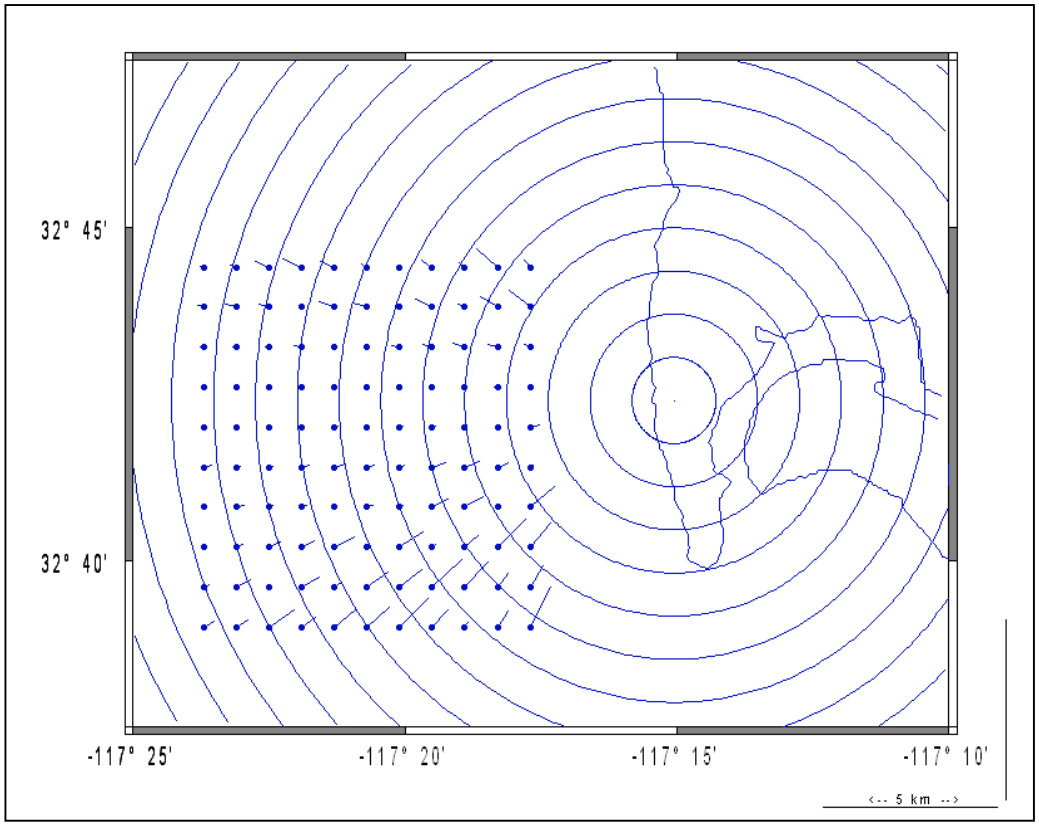

Figure 7. A map of radial currents derived from eight range bins of data using 50% range overlap, then resampling to a fixed lat-long grid, shows deep water flow different from the wind driven uni-directional surface flow.

In Fig. 6, near the surface, one sees positive or approaching radial currents with –36^{o} as the minimum, indicating this bearing is closest to perpendicular to the upwind direction. The 24^{o} azimuth shows maximum surface layer shift, indicating the direction nearest upwind. We found that the shallowest water radial current results versus radar bearing shows a cosine dependence centered on 210^{o}. Thus, our estimate of the surface current at 40-cm depth is 42 cm/s, from a direction of 210^{o}.

Data were collected for four range bins spanning roughly 8 km, and these were resampled to a latitude-longitude grid of equal spacing to provide a plan view of the current field for a single fixed depth from the set shown in the previous figure. This allows one to see the rotational structure in greater detail in Figure 7. As these data were for a ship tracking experiment, we were limited to a total of just four range bins using 32 frequencies. However, using the Octopus transceiver unit, we can now basically map over tens of kilometers using 32 frequencies. While we cannot identify the source of the deep water currents from just a single set of ratial components, one might speculate either an offshore eddy or a bend in a current stream just offshore. The important thing is that mutiple frequencies allow both surface effects and deep water flow to be identified when they are different. Addionally, a radar operating in the 12-20 MHz range would be sampling in the confused transition region and not gain any useful information from the area, with no knowledge of the true flow field that presents itself with such a current shear profile as is presented here.

SUMMARY

We have discussed the scales associated with different current field sources in coastal processes, and the radars that can measure these processes. The current field scales range from 10 to 1,000 m, and we showed how radars operating at microwave and HF frequencies can be used to span these scales. The VHF band alluded to in the introduction is being developed for the 100-m scale, and will operate in a bistatic mode. We discussed new digital transceiver technology, and how this has been adapted to radar development for these three radar types. A method was described and examples were shown of measurement of ocean wave spectra using a non-coherent marine radar. At HF, multiple frequency examples were shown of a small boat radar cross section dependence, and how this might be used as a classification tool, including bistatic illuminating sources. Similar data were uses to measure current shear using the HF band, with the observation of wind driven current shear in the upper layer masking the current field of a water eddy below 1-m depth.

We currently have under development a coherent microwave radar that will be able to map rip currents at the 10-m scale. As each radar only measures a radial velocity component along its look direction, two or more radars are required spaced ~500 m along the beach to map vector currents. This radar design will be tested in the spring of 2006 and results should be

available before the end of that calendar year.

A fourth radar, operating in the 50-75 MHz band, will cover the mid scale and complete the goal of covering the three remote sensing scales discussed in the introduction : 10, 100, and 1,000 m cell sizes. This sytem will cover ranges out to ~ 10 km according to current design, primarily in the line-of-sight mode, and will be quite compact compared to the HF radar. This system is currently in development at our FRF field site, Duck, NC. For more information on any of these radars or operational concepts, contact us at dennis@isr-sensing.com.

REFERENCES

[1] Dankert H., J. Horstmann, and W. Rosenthal, Ocean Wind Fields Retrieved from Radar-Image Sequences, J. Geophys. Res.. Vol. 108, doi: 10.1029/2003JC002056, 2003

[2] Trizna, D.B., Errors in Bathymetric Retrievals using Linear Dispersion In 3D FFT Analysis of Marine Radar Ocean Wave Imagery, IEEE Trans. Geosciences and Remote Sensing, **39**, pp. 2465-2469, 2001.

[3] Bogle, R.W. and D.B. Trizna, Small Boat HF Radar Cross Section, NRL Memo Report 3322, July 1976

[4]. Teague, C.C. (1986), Multifrequency HF radar observations of currents and current shears, IEEE J. of Oceanic Engr., vol. OE-11, pp. 258-269.

[5]. Fernandez, D.M., J.F. Vesecky and C.C. Teague (1996), Measurements of upper ocean surface current shear with high-frequency radar, J. Geophys. Res., 101, pp. 28,615-28,625.

[6]. Calvin C. Teague, John F. Vesecky, and Zackariah R. Hallock, ``A comparison of multi-frequency HF radar and ADCP measurements of near-surface currents during COPE-3," *IEEE Journal of Oceanic Engineering*, vol. 26, no. 3, pp. 399-405, July 2001.